Heterologously Expressed GLT-1 Associates in ~200-nm Protein-Lipid Islands

Stefan Raunser,* Winfried Haase,* Cornelia Franke,† Gunter P. Eckert,† Walter E. Müller,† and Werner Kühlbrandt*

*Department of Structural Biology, Max-Planck-Institute of Biophysics, Frankfurt am Main, Germany; and †Department of Pharmacology, Biocenter Niederursel, University of Frankfurt, Frankfurt am Main, Germany

ABSTRACT The glutamate transporter GLT-1 from *Rattus norvegicus* was expressed at high level in baby hamster kidney (BHK-21) cells by the Semliki Forest Virus expression system. We examined the expressed GLT-1 in the plasma membrane and found that the transporter accumulates in detergent-insoluble lipid-protein assemblies. Freeze-fracture, immunogold labeling, and electron microscopy revealed that GLT-1 forms ~200-nm protein-rich islands in the plasma membrane. Cholesterol depletion in living cells resulted in a dispersion of the GLT-1 islands, indicating that they are the result of lipid-protein rather than protein-protein interactions. Disruption of GLT-1 islands and dispersion of GLT-1 goes along with a reduction of the glutamate transport activity. Our direct visualization of lipid-protein islands in the plasma membrane of tissue culture cells suggests that the reported clustering of glutamate transporters and their cholesterol-dependent transport activity in cells is likewise connected to their association with cholesterol-rich microdomains in the plasma membrane.

INTRODUCTION

Glutamate is the major excitatory neurotransmitter in mammalian brain. The concentration of glutamate in the synaptic cleft is regulated by secondary glutamate transporters, which maintain an extracellular concentration below neurotoxic levels (1–5). The uptake process is electrogenic (6–8), involving the cotransport of three sodium ions, one proton, and one glutamate molecule, and the countertransport of one potassium ion (9–11).

Of the five eukaryotic glutamate transporters identified and cloned so far (GLT-1 (10), GLAST-1 (12), EAAC-1 (13), EAAT4 (14), EAAT5 (15)), GLT-1 is localized almost exclusively to astrocytic plasma membranes, with a much higher density of GLT-1 in membrane areas oriented to the synaptic cleft than in other areas (16).

Several mechanisms have been proposed for the post-translational regulation of glutamate transporters. For EAAC-1 it was shown that glutamate transport in African green monkey kidney (COS) cells is rapidly increased after activation with PKC and that this is due to mobilization of EAAC from intracellular stores (17,18). In contrast to EAAC-1, no significant intracellular concentrations of GLAST-1 and GLT-1 have so far been detected in brain astrocytes, indicating that these proteins are mostly found on the cell surface (19). Other experiments have indicated that glutamate transporters are regulated by a redox mechanism (20), by phosphorylation (21), or through the action of arachidonic acid (22).

The lipid environment of glutamate transporters is important for their activity. Experiments with GLT-1 reconstituted into proteoliposomes indicated that cholesterol is required for Na^+-dependent [^{3}H]-L-glutamate uptake (23). In addition, it has been shown that clustered GLT-1 is associated with detergent-resistant membranes (DRM) isolated from brain tissue (24). DRMs resemble the lipid-protein microdomains of the plasma membrane, also called lipid rafts that are enriched in cholesterol and glycosphingolipids (25). These cholesterol/sphingolipid-rich microdomains (CSRM) are present in the plasma membrane of neurons as well as in glia cells and are important in a variety of functions, especially signal transduction (25). A dynamic assembly of glutamate transporters in CSRMs offers a suitable mechanism for regulating the glutamate transport activity with an unchanged copy number of transporters in the membrane.

We show here that glutamate transporter GLT-1 heterologously expressed in BHK cells enriches in DRMs and associates with CSRMs in the plasma membrane. Immunogold labeling and freeze-fracture electron microscopy reveals that the transporter clusters in 200-nm lipid-protein microdomains in the plasma membrane. Cholesterol depletion causes a disruption of the GLT-1 microdomains and a concomitant reduction of glutamate transport activity.

MATERIALS AND METHODS

Strains and cell culture

Escherichia coli strain XL-1blue (Stratagene, La Jolla, CA) was used for subcloning and propagation of recombinant plasmids. Semliki Forest virus (SFV) was produced in the adherently growing baby hamster kidney cell line BHK-21 [C-13] (ATTC, Manassas, VA). Another BHK-21 [C-13]-2P cell line (ECACC, Salisbury, United Kingdom) was used routinely for the expression of recombinant GLT-1 transporter genes. BHK-21 [C-13]-2P

Submitted April 12, 2006, and accepted for publication August 14, 2006.

Address reprint requests to Dr. Werner Kühlbrandt, Dept. of Structural Biology, Max-Planck-Institute of Biophysics, Max-von-Laue-Str. 3, 60438 Frankfurt am Main, Germany. E-mail: werner.kuehlbrandt@mpibp-frankfurt.mpg.de.

0006-3495/06/11/3718/09 $2.00

doi: 10.1529/biophysj.106.086900

cells adapted to growth in suspension culture were grown in Glasgow-MEM (modified Eagles medium) medium (Sigma-Aldrich, St. Louis, MO) supplemented with 2 mM glutamine (Sigma-Aldrich), 5% tryptose phosphate broth (Sigma-Aldrich), 10% fetal calf serum (PAA, Pasching, Austria) and 1% penicillin/streptomycin-mix (100×) (Sigma-Aldrich). All cells were maintained in a humidified atmosphere with 5% CO_2 at 37°C.

High-yield expression of GLT-1 in BHK-21 cells

Recombinant Semliki Forest virus particles containing the GLT-1 gene were generated as described in detail elsewhere (26). Briefly, linearized DNA was purified with Microspin S-200 HR gel filtration columns (Amersham, Piscataway, NJ) before in vitro transcription. For RNA transcription 70 U SP6 RNA polymerase (Fermentas, Burlington, Canada) and 1 mM m7′G(5′)ppp(5′)G Cap analog (New England Biolabs, Ipswich, MA) were used. Electroporation of cells was repeated twice in a BioRad Gene Pulser II (75 μF, 360 V, 10 Ω) with 0.2 cm Gene Pulser cuvettes (BioRad Laboratories, Hercules, CA). 48 h after virus production, the supernatant of the cells was collected and passed through a 0.22-μm sterile filter. The virus suspension was stored in aliquots at −80°C. Virus particles were activated as described (27). For infection of BHK-21 suspension cultures with activated virus particles, the cells were grown to a density of ~70–100 × 10^4 cells/ml, collected by centrifugation and resuspended in fresh medium (~70–100 × 10^5 cells/ml). Activated virus particles were mixed with the cell suspension at the optimal virus titer and incubated at 37°C in a CO_2 incubator. 2 h after infection the cell suspension was diluted with culture medium to a density of 70–100 × 10^4 cells/ml. The cells were cultured for 30 h.

Membrane preparation

Membranes were prepared as described previously (26). Briefly, cells were harvested by centrifugation and washed twice with phosphate buffered saline (PBS). For homogenization cells were resuspended in 0.25 M sucrose, 25 mM HEPES, pH 7.4, 5 mM EGTA supplemented with 1 mM phenylmethanesulfonyl fluoride (PMSF) and 2 μl/ml protease-inhibitor cocktail for mammalian cells (PIM). The cell suspension was passed three times through a microfluidizer. Unbroken cells were removed by centrifugation at 3000 × g and 4°C for 15 min. Membranes were pelleted at 100,000 × g and 4°C for 1 h and resuspended in 50 mM HEPES, pH 7.4, 200 mM NaCl, 2 mM $MgCl_2$, 2 mM EGTA, 20 mM β-mercaptoethanol including 0.1 mM PMSF and 1 μl/ml PIM at a total protein concentration of 20 mg/ml (28). Aliquots were snap-frozen in liquid nitrogen and stored at −80°C.

Transport assays

Uptake of [^{3}H]-L-aspartate (Amersham) was measured as described (29); 20 μl cell suspension was added to 360 μl 150 mM NaCl, 10 mM KP_i, pH 7.4, and 100 nM [^{3}H]-L-aspartate (29 Ci/mmol). Control experiments without a Na^+ gradient were performed using 150 mM choline chloride instead of NaCl or with the nontransportable inhibitor (2S, 4R)-4-methyl glutamate (SYM; Tocris, Bristol United Kingdom). Routinely, assays were terminated after 10 min. Nitrocellulose filters with 0.45 μm pore size were transferred to scintillation vials, mixed with scintillation fluid (Rotiscint eco plus, Roth, Karlsruhe, Germany). [^{3}H]-L-aspartate or [^{3}H]-L-glutamate was determined with a scintillation counter TRI-CARB 1500 (Canberra-Packard, Rissasanga, Canda).

Protein determination, SDS-PAGE, and immunoblot analysis

Membrane protein concentration was determined by the method of Bradford (28) or with a BCA assay kit (Pierce, Rockford, IL). For SDS-PAGE, proteins were separated on a 10% polyacrylamide gel. After electrophoresis the proteins were either stained with Coomassie brilliant blue or electroblotted onto polyvinylidene difluoride membranes (Millipore, Bedford, MA). As primary antibodies polyclonal rabbit anti-GLT-1 antibody (1:1000, Alpha Diagnostic, San Antonio, TX) or mouse antiflotillin antibody (1:250, Transduction Lab., Lexington, MA) was used. Bound antibodies were detected with anti-rabbit IgG or anti-mouse IgG conjugated to alkaline phosphatase. Biotinylated glutamate transporters were detected with alkaline phosphatase streptavidin (Vector Laboratories, Burlingame, CA).

Labeling of cell-surface proteins

Cells were rinsed with ice-cold PBS containing 0.1 mM $CaCl_2$ and 1 mM $MgCl_2$ and were incubated in the same solution supplemented with 1 mg/ml *N*-hydroxysulfosuccinimido biotin (Pierce) for 20 min at 4°C. After incubation, cells were rinsed several times with PBS-Ca/Mg containing 100 mM glycine and incubated in this buffer for 30 min at 4°C to quench the unreacted biotin.

Freeze-fracture analysis

Cells were fixed for 30 min in 2.5% glutaraldehyde in PBS at room temperature and then transferred stepwise to 30% glycerol. A droplet of cell suspension was placed between two copper sheets as sample holders and frozen in ethane cooled with liquid nitrogen. Fracturing and shadowing were carried out in a BAF T400 freeze-fracture machine (Balzers, Liechtenstein) with a pressure of 2 × 10^{-7} mbar, keeping the specimen stage at − 140°C. Pt/C shadowing was performed at an angle of 45° for Pt and 90° for pure carbon. Unfixed BHK cells were used for freeze-fracture immunogold-labeling. Replicas were labeled according to Fujimoto (30). Briefly, the replicas were thawed in 2.5% SDS in 10 mM Tris-HCl and 30 mM sucrose, pH 8.3. After two changes of the SDS solution, replicas were stirred overnight, washed in PBS, and incubated for 2 h with the specific primary antibody (polyclonal rabbit anti-rat GLT-1 protein diluted 1:750 in PBS + 0.1% BSA). To demonstrate binding sites of primary antibodies they were reacted with a secondary gold-marker ligated antibody (goat antirabbit-Gold (10 nm, Amersham). After a washing step, replicas were treated with 1% glutaraldehyde/PBS, washed with water and placed on Formvar coated copper grids for examination in the electron microscope.

Isolation and characterization of detergent-resistant membranes

Detergent-resistant membranes (DRMs) were isolated as described (31) by incubating 40 mg membranes with 1% (v/v) Triton X-100. Alkaline phosphatase was determined as described (32). Flotillin and GLT-1 were determined with SDS-PAGE followed by Western blot analysis with the respective antibodies. The same amount of total protein was used for each fraction. Lipids were extracted with chloroform-methanol (2:1 v/v). The organic phase containing the lipids was recovered and the solvent was removed by rotary evaporation. The extracted lipid was redissolved in chloroform-methanol (2:1 v/v). Samples and standards were spotted on silica gel TLC plates and developed in chloroform-methanol-acetic acid-water (60:50:1:4 v/v). Spots were visualized with iodine vapor. Samples were quantified densitometrically using the Kodak DSIC software package. Cholesterol was determined by a cholesterol/peroxidase based assay (33), using 0.5% (w/v) methyl-β-cyclodextrin in combination with 15% (w/v) Brij 35 instead of sodium cholate.

Cholesterol depletion

Lovastatin (Sigma-Aldrich) was prepared as a 20 mM stock solution as described (34). After infection with virus particles, BHK-21 suspension cells were grown in medium containing 4 μM lovastatin and 0.25 mM mevalonate for 30 h. The cells were pelleted and resuspended in medium supplemented with 10 mM methyl-β-cyclodextrin. After treatment for

30 min at 37°C, the cells were washed several times in PBS and used for aspartate/glutamate uptake measurements or freeze-fracture analysis.

RESULTS

Plasma membranes of BHK-21 cells overproducing GLT-1 were analyzed by freeze-fracture electron microscopy. This revealed ~200 nm islands of densely packed protein (Fig. 1 *A*). The average diameter of the protein particles in the island was ~10 nm, in good agreement with the size of the GLT-1 complex (26). In control cells infected with empty SFV particles not containing the GLT-1 gene, these protein islands were absent (Fig. 1 *B*). Immunogold-labeling of freeze-fracture replicas with anti-GLT-1 primary antibody demonstrated that the membrane protein in the densely packed islands was indeed GLT-1 (Fig. 1 *C*). The microdomains were not associated with invaginations in the membrane. We also used different SFV titers to alter the GLT-1 expression level (data not shown). The size of the protein patches did not depend on the GLT-1 expression level. However, the total number of observed protein islands decreased at reduced protein expressions. We assumed that these protein islands were associated with CSRMs of the membrane.

To verify this assumption, we used a routine procedure (35) to extract detergent-insoluble fractions from BHK-21 plasma membranes containing GLT-1-with 1% Triton X-100 at 4°C and flotation on a sucrose density gradient. As a control, we used membranes of cells that had been infected with virus particles not containing the GLT-1 gene.

The DRM fractions were isolated by density gradient centrifugation and identified in several ways (Fig. 2). Strong light scattering at 620 nm served as a first characteristic (36) (Fig. 2 *A*). Most of the light-scattering material was found in fraction 6, which also had the highest protein concentration (Fig. 2 *B*). The characteristic detergent-resistant lipids, cholesterol and sphingomyelin, were enriched in this fraction (Fig. 2, *C* and *E*). GPI anchored proteins, such as alkaline phosphatase and flotillin are well-known marker proteins of DRMs (37). To determine the accumulation of these proteins, the enzyme activity of alkaline phosphatase was measured (Fig. 2 *D*) and the distribution of flotillin in the fractions of interest was determined by Western blot analysis (Fig. 2 *F*). Both alkaline phosphatase and flotillin were highly enriched in fraction 6. Taken together these results indicate clearly that fraction 6 contained DRMs.

No significant difference was observed between samples with and without GLT-1. The DRM fraction was freeze-fractured and analyzed by electron microscopy (Fig. 1 *D*). The main constituents were large multilayered membrane vesicles, which apparently had formed after isolation by fusion of rafts in the presence of detergent. The vesicles contained high levels of protein and measured several micrometers in diameter. The protein distribution in the vesicle membranes was uneven. In most vesicles, membrane proteins were

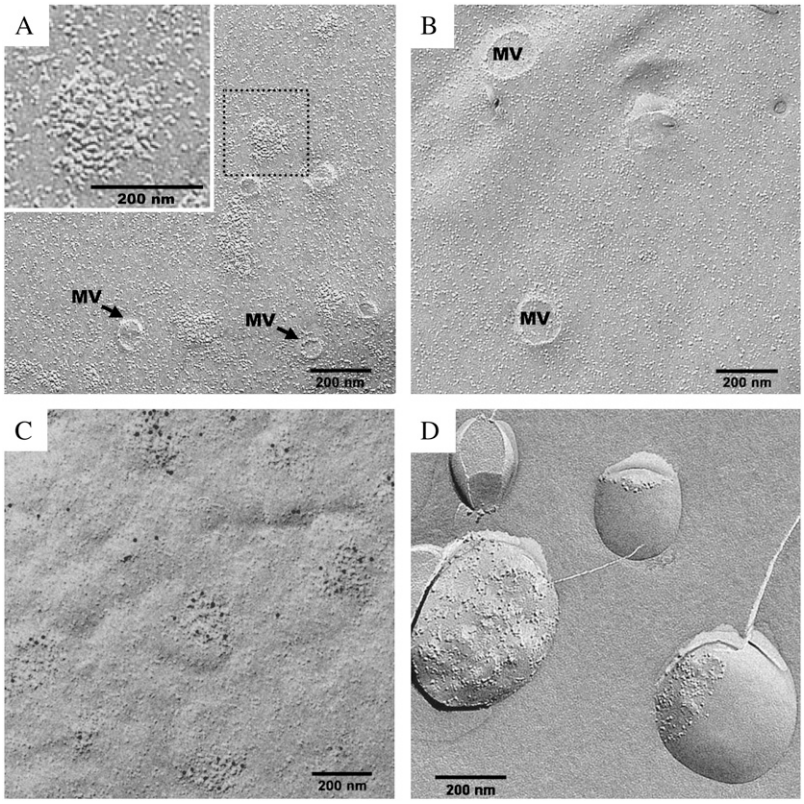

FIGURE 1 GLT-1 assembles into protein-rich islands in the plasma membrane, as shown by freeze-fracture electron microscopy. (*A*) Plasma membrane of BHK-21 cells infected with SFV containing the GLT-1 gene. (*Inset*) Boxed area at higher magnification, showing a typical GLT-1 island. (*B*) Plasma membrane of control cells infected with SFV not containing the GLT-1 gene. (*C*) Immunogold labeling with anti-GLT-1 antibody of freeze-fracture replicas from unfixed cells. (*D*) Isolated lipid rafts containing GLT-1 (fraction 6) form single-walled vesicles in which protein-rich clusters are laterally segregated from large protein-free membrane areas. MV, sheared-off microvilli.

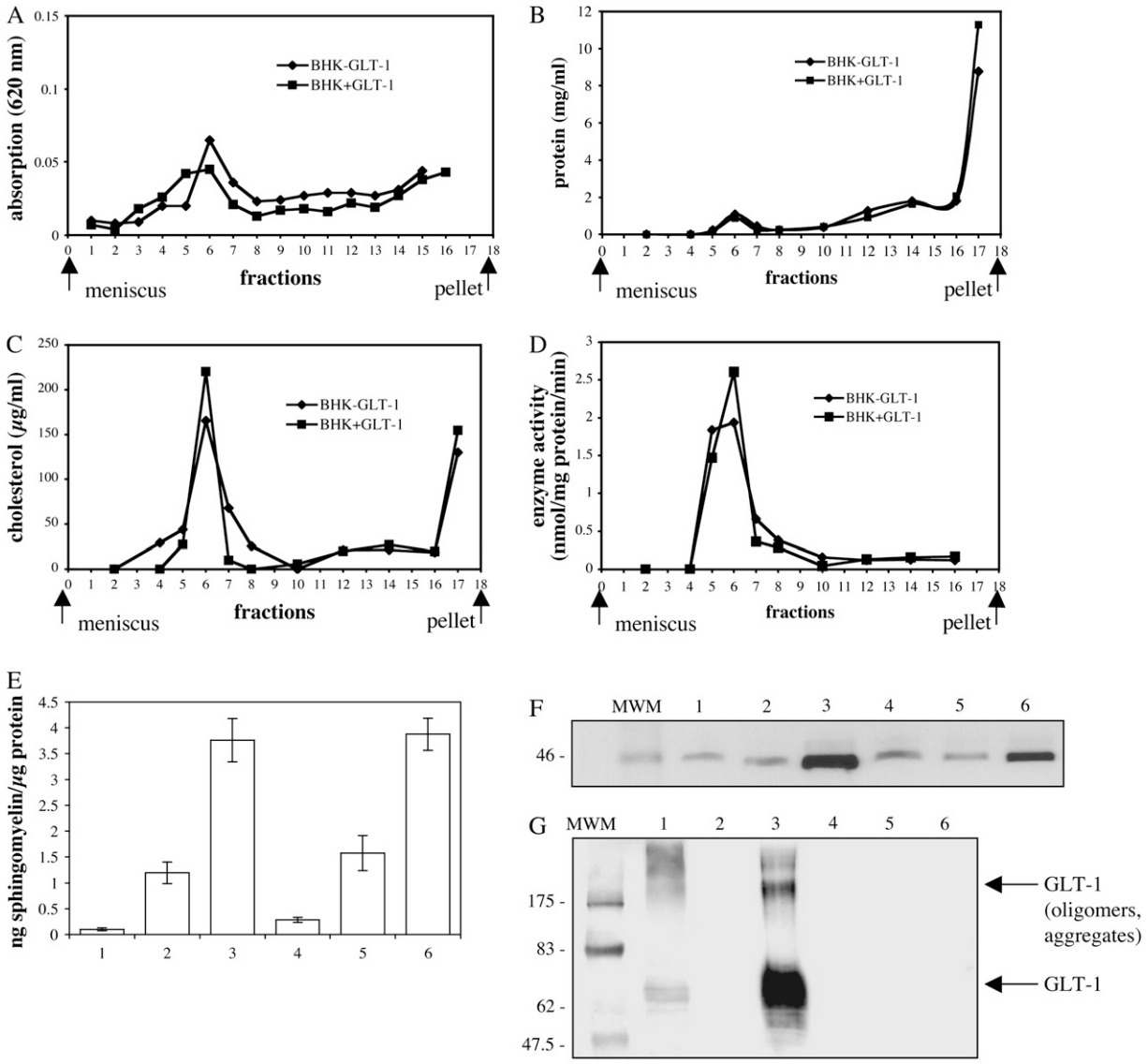

FIGURE 2 Sucrose gradient fractions of DRMs. DRMs were extracted with 1% Triton X-100 from membranes of BHK-21 cells either expressing or not expressing GLT-1. The raft fraction was isolated by flotation on a sucrose gradient; 2 ml fractions were collected from the top. (*A*) Absorption at 620 nm; (*B*) total protein content (mg/ml), measured with BCA; (*C*) cholesterol content (μg/ml); (*D*) alkaline phosphatase activity (nmol/mg protein/min). (*E*) Sphingomyelin content of protein-containing fractions as determined by thin-layer chromatography. The distribution of the marker protein flotillin (*F*) and GLT-1 (*G*) was determined by SDS-PAGE and Western blot. The same amount of total protein was applied to each lane. (*E–G*) Fractions 17, 10, and 6 of BHK cells expressing GLT-1 (*lanes 1–3*); fractions 17, 10, and 6 of BHK cells not expressing GLT-1 (*lanes 4–6*).

found exclusively in tightly clustered protein-lipid domains continuous with large protein-free lipid areas. Western blot analysis with anti-GLT-1 antibody (Fig. 2 *G*) showed that the glutamate transporter GLT-1 was highly enriched in the DRM fraction (Fig. 2 *G*, *lane 3*), whereas no GLT-1 was found in the control DRMs (Fig. 2 *G*, *lane 6*), as expected. These experiments indicate that the expressed GLT-1 accumulates in DRMs. However that does not prove that the clustering of GLT-1 in protein islands we observed is due to an interaction with lipids in CSRMs in the plasma membrane, even if the lipid composition of these domains resembles those of DRMs. To demonstrate the localization of GLT-1 in CSRMs, we decided to disrupt the GLT-1 protein islands in living cells.

CSRMs can be disrupted in vivo by reducing the amount of cholesterol in the membranes, using a combination of two different effects (38). First, the de novo synthesis of cholesterol in the ER is inhibited by lovastatin in the presence of small amounts of mevalonate to allow for the synthesis of nonsterol products (39). Second, cholesterol is extracted from the plasma membrane using methyl-cyclodextrin. Treatment with lovastatin alone reduces the cholesterol levels only by 10% but it increases the effect of methyl-cyclodextrin. The combination of the two methods makes it possible to reduce

cholesterol in the plasma membrane of BHK cells by 60% without affecting ER-to-Golgi transport (38).

BHK cells overproducing GLT-1 were treated with lovastatin/mevalonate for 30 h after infection. Cholesterol was extracted with 10 mM methyl-β-cyclodextrin for 30 min immediately before the cells were used for aspartate/glutamate uptake measurements or freeze-fracture. Control cells were grown without lovastatin/mevalonate and not treated with methyl-β-cyclodextrin.

Cells grown in lovastatin/mevalonate showed a normal growth rate compared to control cells (Fig. 3 *A*). Trypan blue staining proved that the cells were viable after depletion of cholesterol. Transport of aspartate/glutamate into intact BHK cells was significantly reduced by 30% upon cholesterol extraction (Fig. 3 *B*). The observed change in transport activity may result either from a reduction in the number of GLT-1 molecules in the plasma membrane or from a decrease in the turnover rate of the transporters.

To discriminate between these two possibilities, we incubated cells grown in lovastatin/mevalonate and control cells in *N*-hydroxysulfo-succinimido biotin to biotinylate surface proteins. Membranes were prepared and GLT-1 was purified with a Ni-NTA column. The eluate was then analyzed by SDS-PAGE and by Western blotting. There was no difference in the surface expression level of GLT-1 compared to control cells (data not shown). Therefore the observed reduction of glutamate/aspartate transport after cholesterol depletion was caused by a change in the turnover number and not by a decrease in the copy number of transporter molecules on the cell surface. Freeze-fracture analysis and electron microscopy revealed that the characteristic GLT-1 transporter islands had disappeared in the cells with reduced cholesterol content (Fig. 3 *C*) whereas they were present in control cells. The proteins were distributed equally in the plasma membrane. Since activity tests of cells with GLT-1 patches indicated a higher rate of aspartate/glutamate uptake than those without patches, we can exclude the possibility that the protein islands were aggregates of inactive protein.

As an additional, unexpected effect, smooth, protein-free lipid areas appeared in most of the membranes after cholesterol depletion (Fig. 3 *D*). These smooth areas were apparently due to a partial lateral segregation of lipid and protein in the cell membrane.

In summary, a depletion of CSRMs in the membrane by the reduction of cholesterol resulted in a disaggregation of the GLT-1 transporter islands that went along with a reduction of aspartate/glutamate transport activity.

DISCUSSION

Our results show that heterologously expressed glutamate transporter GLT-1 assembles into CSRMs in the plasma membrane of BHK-21 cells. The diameter of the CSRMs as determined from the size of the GLT-1 islands in freeze-fracture replica was ~200 nm. Depending on the method used, the postulated size of CSRMs, also called lipid rafts

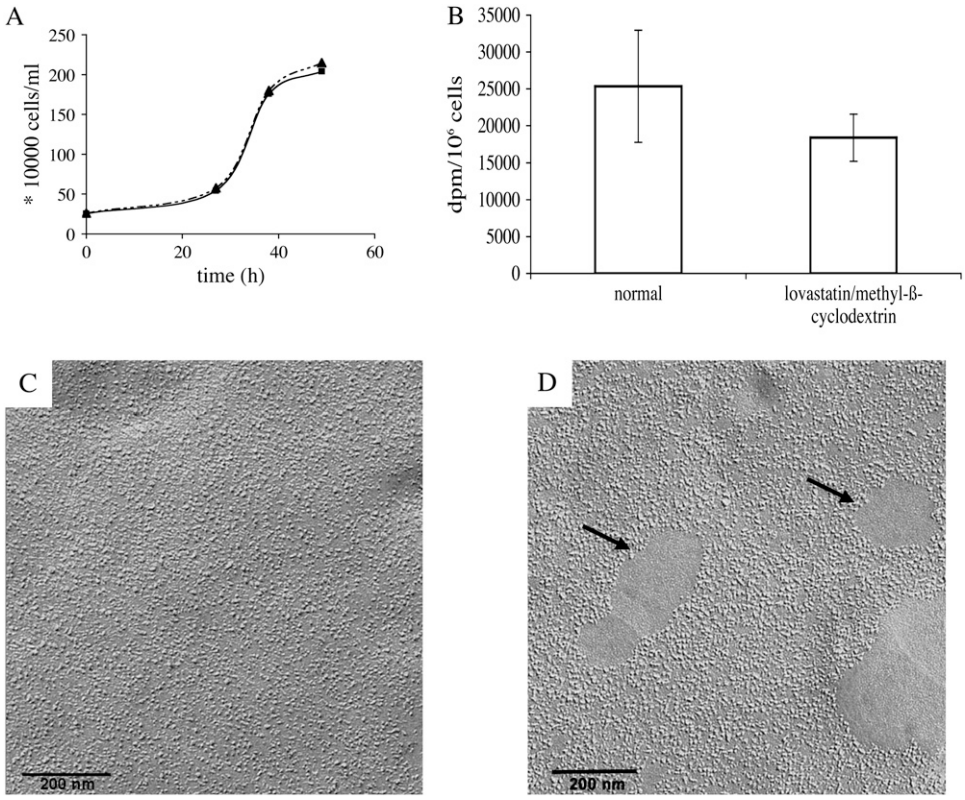

FIGURE 3 Depletion of cholesterol from the plasma membrane in living cells (*A*). Growth curves of BHK cells in the presence of (■) and without (▲) lovastatin/mevalonate. (*B*,*C*) BHK suspension cells grown with or without lovastatin/mevalonate were infected with the same amount of SFV and harvested after 30 h. After washing in PBS the cells treated with lovastatin/mevalonate were incubated with 10 mM methyl-β-cyclodextrin in PBS for 30 min and the uptake of [^{3}H]-L-aspartate in the BHK cells was determined (*B*) or the cells were freeze-fractured and examined in the electron microscope (*C*,*D*). The data in panel *B* represent the mean of five separate experiments. Plasma membranes of lovastatin/mevalonate-treated cells did not show the characteristic GLT-1 islands but a more or less uniform protein distribution (*C*). However, most membranes of cells treated in this way exhibited protein-free lipid patches (*arrows* in *D*).

ranges from a few molecules to ~700 nm. For instance, homo and hetero FRET-based experiments revealed that most GPI-anchored proteins in live cells are present mostly as monomers and as nanoscale (<5 nm) cholesterol-sensitive clusters (40). However, lipid rafts of 0.7 μm size were found in native muscle cell membranes using single molecule microscopy (41). The GLT-1 protein-lipid islands described here are in the middle of this size range.

The GLT-1 islands were not associated with invaginations in the membrane. Depletion of cholesterol from the plasma membrane resulted in a disruption of the CSRMs and therefore of the GLT-1 islands. This coincided with a ~30% reduction in glutamate transport activity.

The assembly of the protein in clusters might simply be a side effect of the high-level expression of GLT-1. However, the massive overexpression (3.5×10^6 transporters/cell or ~11,200 transporters/μm^3, assuming a diameter of 10 μm for a BHK-21 cell) (26) resembles the expression level of the glutamate transporter GLT-1 in hippocampal tissue (12,000 transporters/μm^3 hippocampus) (42). In natural tissue, in particular in neurons and astrocytes, the glutamate transporter is also found in clusters that undergo rapid morphological changes in both shape and size (16,43–45). It was suggested that the morphogenesis of GLT-1 clusters is dependent on the actin network and that their dynamic formation plays an important role in regulating glutamate uptake (44). Indeed, protein-lipid microdomains of the size we observe probably require a scaffolding protein to link the GLT-1 transporters together. In glia cells, the LIM-protein Ajuba has been proposed to anchor the glutamate transporters to the cytoskeleton (46). Our results indicate however that GLT-1 clustering is not only due to protein-protein interaction but also to lipid-protein interaction.

Recently it was shown that GLT-1 in cortical astrocytes is organized in DRMs (24,47), which were isolated either without detergent (47) or by extraction with the detergent Brij-58 (24). In contrast to our results, GLT-1 was soluble in Triton X-100. The fact that GLT-1 forms clusters in the membrane in kidney cells, which do not naturally contain high levels of glutamate transporters, proves that this is an inherent property of the transporter and not specific to glia or nerve cells.

Extraction of DRMs is a method often used for analyzing possible CSRM association of proteins. The detergent disrupts lipid-protein interactions, so that most membrane proteins are solubilized. Association of a protein in DRMs is indicative of a strong interaction with tightly packed domains in the cholesterol- and sphingolipid-rich I_o phase (48). The isolation of DRMs with different detergents as a characterization of native CSRMs in cell membranes has been debated recently. It was shown that the presence of proteins or lipids in DRMs obtained with a particular detergent does not necessarily indicate association with the same domains in the native membrane (49). In addition, it was reported that Triton X-100 used most frequently in these studies may induce large-scale ordered domains in lipid vesicles that are in turn resistant upon subsequent membrane solublization (50). However, isolation of DRMs is still accepted as a valuable tool for the analysis of biological membranes including cholesterol-sphingolipid rich microdomains (49) and proves a high biochemical affinity of proteins localized in DRMs for the lipids that characterize these domains.

Our results show that the reduction of glutamate transport is caused by the disruption of the CSRMs and a redistribution of the transporter in the membrane. The clustering must be mediated by cholesterol-protein interaction, because membranes containing the same level of GLT-1 but only 40% of the normal cholesterol level do not show the characteristic protein microdomains as suggested in Fig. 4. We can therefore exclude direct interaction of the glutamate transporters themselves as the cause of GLT-1 microdomain formation.

Cholesterol depletion is a common method for disrupting CSRMs in vivo (38). Recently it was reported that depletion of cell cholesterol can have global effects on cell and plasma membrane architecture and function. In one case (51), cholesterol depletion resulted in a reduced lateral mobility of membrane proteins due to a reorganization of the actin cytoskeleton. By contrast, our observations and those of other laboratories (52) indicate that cholesterol depletion leads to a rapid and complete redistribution of CSRM proteins in the membrane.

Our observations contrast with those of glutamate transporters in rat primary brain cortical cultures that showed a reduction of surface EAAT2 levels after depletion of cholesterol. Butchbach et al. suggested that a depletion of membrane cholesterol reduces the localization of the EAAT2 to the cell surface by endocytosis of the human GLT-1 homolog

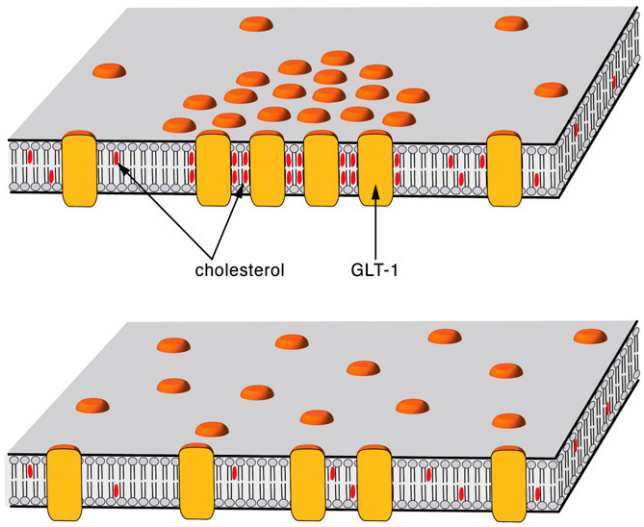

FIGURE 4 Proposed mechanism of activity regulation of GLT-1 by cholesterol-induced association of GLT-1 into microdomains and their dispersion upon cholesterol depletion. Clustering of GLT-1 is caused by specific cholesterol binding to GLT-1, rather than by direct protein-protein interaction. Low cholesterol levels prevent this interaction.

EAAT2 (24). The observations that most GLAST-1 and GLT-1 in brain astrocytes are found on the cell surface (19) corroborate our results. Another argument against the endocytosis hypothesis is that GLT-1 patches do not colocalize with membrane invaginations. We conclude from this observation that GLT-1 does not associate with caveolar lipid rafts. Caveolae are formed from lipid rafts by polymerization of caveolins. They form flask-shaped plasma membrane invaginations and are involved in endocytosis (53,54). A coimmuno-localization study with antibodies directed against caveolin-1 and GLT-1 in astroglial cells also showed that GLT-1 is not located in caveolar lipid rafts (47).

Normally, it is difficult to visualize CSRMs directly. First, their relatively small size (up to a few 100 nm) makes it difficult to examine them under the light microscope. Fluorescence-based approaches are relatively indirect. Second, the density and concentration of the microdomain-associated proteins is low. We present here the first direct observation by freeze-fracture electron microscopy of CSRMs connected to the natural assembly of proteins in the membrane. In principle, electron microscopy is a suitable technique for visualizing membrane domains in live cells but there are few reports of this in the literature. Some signaling proteins have been mapped by electron microscopy, although this was limited to morphologically identifiable plasma membrane structures such as caveolae (55,56) or osmiophilic patches (57,58). A recent report combined immunogold electron microscopy with a statistical analysis of gold patterns to visualize microdomain-resident proteins directly at high resolution (52,59).

Normally, larger areas that can be examined by electron microscopy are produced only after cross-linking of CSRM proteins with antibodies (25). Evidently, the GLT-1 transporter has a much stronger tendency to cluster than GPI-anchored proteins or other characteristic CSRM proteins. The reason for the strong interaction of GLT-1 in the membranes must be the attractive force between the proteins and surrounding lipids. A similar concentration of proteins in the membranes was observed with glutamate receptors in neurons of the neocortex and described as hot spots (60). It was also postulated that AMPA receptors localize in lipid rafts (61). A depletion of cholesterol/sphingolipids lead to instability of surface AMPA receptors in neurons and gradual loss of synapses.

Smooth, protein-free areas of ~200-nm size were observed in the membrane after cholesterol depletion. Similar large, particle-free smooth patches have been described before in unfixed mitochondrial and nuclear membranes (62–64). It was found that temperatures below 10°C before freezing induced a lateral segregation of membrane proteins and lipids into small protein-free lipid patches surrounded by large membrane areas with a more or less even protein distribution. This does not occur if the membranes are fixed at room temperature or ~37°C (64). Although we fixed the cells at room temperature before freezing, we observed lateral lipid-protein segregation in cholesterol-depleted cells. Control cells not subjected to cholesterol depletion did not show this striking effect. Since otherwise the same conditions were used in all experiments, this effect must be due to methyl-cyclodextrin treatment and cholesterol depletion. These physical changes in the membrane might reflect loss of fluidity at room temperature giving rise to lateral segregation of lipid and protein, which occurs only at lower temperatures in normal cells (65,66). A similar effect was observed in giant unilamellar vesicles, in which bilayers of lipid mixtures can separate laterally into coexisting liquid phases or domains with distinct lipid compositions (67). At low cholesterol concentration, solid, noncircular domains occur that have a high melting point and that do not self-assemble (68). These rigid lipid patches are probably due to strong lipid-lipid interactions which would tend to expel interspersed protein molecules. Physiological levels of cholesterol thus apparently prevent the formation of protein-free lipid patches in the plasma membrane at room temperature.

Functional significance of GLT-I association with CSRMs

In the bilayer of the membrane, many membrane proteins are thought to be surrounded by a more or less tightly bound shell of lipids (69). If a protein predominantly binds cholesterol and glycosphingolipids, it would tend to form clusters in the membrane, especially at high concentration. Therefore the GLT-1 clusters do not necessarily have a functional role.

However, the density of glutamate transporters in astroglial cells is much higher in regions of the plasma membrane that are oriented to the synaptic cleft than in other areas (16). Assuming the same uneven distribution of lipids in the plasma membrane of glia cells that was found in epithelial cells (70), an association of glutamate transporters with CSRMs would enable their controlled trafficking to cholesterol and sphingomyelin-rich parts of the plasma membrane. The dynamic assembly of GLT-1 into CSRMs and the colocalization with cholesterol is likely to play a role in the regulation of the transporter activity. Cholesterol is important for the activity of the GLT-1 transporter as was shown by proteoliposome reconstitution experiments (23) in which cholesterol depletion reduced the GLT-1 activity. A cholesterol-related regulation was also found for the expression and activity of neuronal EAAC1 which are both regulated by cholesterol (71). Experiments with other neuronal cholesterol-regulated transporters such as the serotonin transporter SERT-1 revealed that it is dynamically associated with CSRMs. The affinity of the transporter to serotonin was not dependent on cholesterol, whereas the transport efficiency depended on cholesterol bound to the transporter (72,73). Likewise, the activity of the metabotropic glutamate receptor in *Drosophila melanogaster* (74) and the rat GABA transporter (23) has been shown to depend on cholesterol. This receptor is also associated with CSRMs (75).

Another reason for the dynamic association of glutamate transporters with CSRMs may be their regulation by activators or inhibitors that colocalize in the same microdomains. It was reported that GLT-1 is directly regulated by arachidonic acid that is localized in CSRMs (22,76). Likewise, protein kinase C that has been reported to regulate glutamate transporters via direct phosphorylation (21) is also associated with CSRMs (25).

Taken together, our findings suggest that glutamate uptake via glutamate transporters in glia cells is controlled by the dynamic assembly of the transporters in CSRMs rather than by a reduction of glutamate transporters on the cell surface by endocytosis.

This work was supported by a PhD fellowship of ''Studienstiftung des deutschen Volkes''.

REFERENCES

1. Kanner, B. I., and S. Schuldiner. 1987. Mechanism of transport and storage of neurotransmitters. Review 223 refs. *CRC Crit. Rev. Biochem.* 22:1–38.
2. Nicholls, D., and D. Attwell. 1990. The release and uptake of excitatory amino acids. *Trends Pharmacol. Sci.* 11:462–468.
3. Zerangue, N., and M. P. Kavanaugh. 1996. Flux coupling in a neuronal glutamate transporter. *Nature.* 383:634–637.
4. Rothstein, J. D., M. Dykes-Hoberg, C. A. Pardo, L. A. Bristol, L. Jin, R. W. Kuncl, Y. Kanai, M. A. Hediger, Y. Wang, J. P. Schielke, and D. F. Welty. 1996. Knockout of glutamate transporters reveals a major role for astroglial transport in excitotoxicity and clearance of glutamate. *Neuron.* 16:675–686.
5. Tanaka, K., K. Watase, T. Manabe, K. Yamada, M. Watanabe, K. Takahashi, H. Iwama, T. Nishikawa, N. Ichihara, T. Kikuchi, S. Okuyama, N. Kawashima, et al. 1997. Epilepsy and exacerbation of brain injury in mice lacking the glutamate transporter GLT-1. *Science.* 276:1699–1702.
6. Kanner, B. I., and I. Sharon. 1978. Active transport of L-glutamate by membrane vesicles isolated from rat brain. *Biochemistry.* 17:3949–3953.
7. Brew, H., and D. Attwell. 1987. Electrogenic glutamate uptake is a major current carrier in the membrane of axolotl retinal glial cells. *Nature.* 327:707–709.
8. Wadiche, J. I., S. G. Amara, and M. P. Kavanaugh. 1995. Ion fluxes associated with excitatory amino acid transport. *Neuron.* 15:721–728.
9. Kanner, B. I., and A. Bendahan. 1982. Binding order of substrates to the sodium and potassium ion coupled L-glutamic acid transporter from rat brain. *Biochemistry.* 21:6327–6330.
10. Pines, G., and B. I. Kanner. 1990. Counterflow of L-glutamate in plasma membrane vesicles and reconstituted preparations from rat brain. *Biochemistry.* 29:11209–11214.
11. Kavanaugh, M. P., A. Bendahan, N. Zerangue, Y. Zhang, and B. I. Kanner. 1997. Mutation of an amino acid residue influencing potassium coupling in the glutamate transporter GLT-1 induces obligate exchange. *J. Biol. Chem.* 272:1703–1708.
12. Storck, T., S. Schulte, K. Hofmann, and W. Stoffel. 1992. Structure, expression, and functional analysis of a Na^+-dependent glutamate/aspartate transporter from rat brain. *Proc. Natl. Acad. Sci. USA.* 89: 10955–10959.
13. Kanai, Y., and M. A. Hediger. 1992. Primary structure and functional characterization of a high-affinity glutamate transporter. *Nature.* 360: 467–471.
14. Fairman, W. A., R. J. Vandenberg, J. L. Arriza, M. P. Kavanaugh, and S. G. Amara. 1995. An excitatory amino-acid transporter with properties of a ligand-gated chloride channel. *Nature.* 375:599–603.
15. Arriza, J. L., S. Eliasof, M. P. Kavanaugh, and S. G. Amara. 1997. Excitatory amino acid transporter 5, a retinal glutamate transporter coupled to a chloride conductance. *Proc. Natl. Acad. Sci. USA.* 94: 4155–4160.
16. Chaudhry, F. A., K. P. Lehre, M. van Lookeren Campagne, O. P. Ottersen, N. C. Danbolt, and J. Storm-Mathisen. 1995. Glutamate transporters in glial plasma membranes: highly differentiated localizations revealed by quantitative ultrastructural immunocytochemistry. *Neuron.* 15:711–720.
17. Dowd, L. A., and M. B. Robinson. 1996. Rapid stimulation of EAAC1-mediated Na^+-dependent L-glutamate transport activity in C6 glioma cells by phorbol ester. *J. Neurochem.* 67:508–516.
18. Davis, K. E., D. J. Straff, E. A. Weinstein, P. G. Bannerman, D. M. Correale, J. D. Rothstein, and M. B. Robinson. 1998. Multiple signaling pathways regulate cell surface expression and activity of the excitatory amino acid carrier 1 subtype of Glu transporter in C6 glioma. *J. Neurosci.* 18:2475–2485.
19. Danbolt, N. C. 2001. Glutamate uptake. Review 1082 refs. *Prog. Neurobiol.* 65:1–105.
20. Trotti, D., B. L. Rizzini, D. Rossi, O. Haugeto, G. Racagni, N. C. Danbolt, and A. Volterra. 1997. Neuronal and glial glutamate transporters possess an SH-based redox regulatory mechanism. *Eur. J. Neurosci.* 9:1236–1243.
21. Casado, M., A. Bendahan, F. Zafra, N. C. Danbolt, C. Aragon, C. Gimenez, and B. I. Kanner. 1993. Phosphorylation and modulation of brain glutamate transporters by protein kinase C. *J. Biol. Chem.* 268:27313–27317.
22. Trotti, D., A. Volterra, K. P. Lehre, D. Rossi, O. Gjesdal, G. Racagni, and N. C. Danbolt. 1995. Arachidonic acid inhibits a purified and reconstituted glutamate transporter directly from the water phase and not via the phospholipid membrane. *J. Biol. Chem.* 270:9890–9895.
23. Shouffani, A., and B. I. Kanner. 1990. Cholesterol is required for the reconstruction of the sodium- and chloride-coupled, gamma-aminobutyric acid transporter from rat brain. *J. Biol. Chem.* 265:6002–6008.
24. Butchbach, M. E., G. Tian, H. Guo, and C. L. Lin. 2004. Association of excitatory amino acid transporters, especially EAAT2, with cholesterol-rich lipid raft microdomains: importance for excitatory amino acid transporter localization and function. *J. Biol. Chem.* 279:34388–34396.
25. Simons, K., and D. Toomre. 2000. Lipid rafts and signal transduction. *Nat. Rev. Mol. Cell Biol.* 1:31–39.
26. Raunser, S., W. Haase, M. Bostina, D. N. Parcej, and W. Kuhlbrandt. 2005. High-yield expression, reconstitution and structure of the recombinant, fully functional glutamate transporter GLT-1 from Rattus norvegicus. *J. Mol. Biol.* 351:598–613.
27. Lundstrom, K. 2003. Semliki Forest virus vectors for large-scale production of recombinant proteins. *Methods Mol. Med.* 76:525–543.
28. Bradford, M. M. 1976. A rapid and sensitive method for the quantitation of microgram quantities of protein utilizing the principle of protein-dye binding. *Anal. Biochem.* 72:248–254.
29. Gordon, A. M., and B. I. Kanner. 1988. Partial purification of the sodium- and potassium-coupled L-glutamate transport glycoprotein from rat brain. *Biochim. Biophys. Acta.* 944:90–96.
30. Fujimoto, K. 1997. SDS-digested freeze-fracture replica labeling electron microscopy to study the two-dimensional distribution of integral membrane proteins and phospholipids in biomembranes: practical procedure, interpretation and application. *Histochem. Cell Biol.* 107:87–96.
31. Eckert, G. P., U. Igbavboa, W. E. Muller, and W. G. Wood. 2003. Lipid rafts of purified mouse brain synaptosomes prepared with or without detergent reveal different lipid and protein domains. *Brain Res.* 962:144–150.
32. Parkin, E. T., I. Hussain, E. H. Karran, A. J. Turner, and N. M. Hooper. 1999. Characterization of detergent-insoluble complexes containing the familial Alzheimer's disease-associated presenilins. *J. Neurochem.* 72:1534–1543.
33. Auerbach, B. J., J. S. Parks, and D. Applebaum-Bowden. 1990. A rapid and sensitive micro-assay for the enzymatic determination of plasma and lipoprotein cholesterol. *J. Lipid Res.* 31:738–742.

34. Fenton, R. G., H. F. Kung, D. L. Longo, and M. R. Smith. 1992. Regulation of intracellular actin polymerization by prenylated cellular proteins. *J. Cell Biol.* 117:347–356.

35. Brown, D. A., and E. London. 1998. Functions of lipid rafts in biological membranes. *Annu. Rev. Cell Dev. Biol.* 14:111–136.

36. Hooper, N. M. 1999. Detergent-insoluble glycosphingolipid/cholesterol-rich membrane domains, lipid rafts and caveolae. *Mol. Membr. Biol.* 16:145–156.

37. Brown, D. A. 1992. Interactions between GPI-anchored proteins and membrane lipids. *Trends Cell Biol.* 2:338–343.

38. Keller, P., and K. Simons. 1998. Cholesterol is required for surface transport of influenza virus hemagglutinin. *J. Cell Biol.* 140:1357–1367.

39. Brown, M. S., and J. L. Goldstein. 1980. Multivalent feedback regulation of HMG CoA reductase, a control mechanism coordinating isoprenoid synthesis and cell growth. *J. Lipid Res.* 21:505–517.

40. Sharma, P., R. Varma, R. C. Sarasij, Ira, K. Gousset, G. Krishnamoorthy, M. Rao, and S. Mayor. 2004. Nanoscale organization of multiple GPI-anchored proteins in living cell membranes. *Cell.* 116:577–89.

41. Schutz, G. J., G. Kada, V. P. Pastushenko, and H. Schindler. 2000. Properties of lipid microdomains in a muscle cell membrane visualized by single molecule microscopy. *EMBO J.* 19:892–901.

42. Lehre, K. P., and N. C. Danbolt. 1998. The number of glutamate transporter subtype molecules at glutamatergic synapses: chemical and stereological quantification in young adult rat brain. *J. Neurosci.* 18:8751–8757.

43. Coco, S., C. Verderio, D. Trotti, J. D. Rothstein, A. Volterra, and M. Matteoli. 1997. Non-synaptic localization of the glutamate transporter EAAC1 in cultured hippocampal neurons. *Eur. J. Neurosci.* 9:1902–1910.

44. Zhou, J., and M. L. Sutherland. 2004. Glutamate transporter cluster formation in astrocytic processes regulates glutamate uptake activity. *J. Neurosci.* 24:6301–6306.

45. Poitry-Yamate, C. L., L. Vutskits, and T. Rauen. 2002. Neuronal-induced and glutamate-dependent activation of glial glutamate transporter function. *J. Neurochem.* 82:987–997.

46. Marie, H., D. Billups, F. K. Bedford, A. Dumoulin, R. K. Goyal, G. D. Longmore, S. J. Moss, and D. Attwell. 2002. The amino terminus of the glial glutamate transporter GLT-1 interacts with the LIM protein Ajuba. *Mol. Cell. Neurosci.* 19:152–164.

47. Zschocke, J., N. Bayatti, and C. Behl. 2005. Caveolin and GLT-1 gene expression is reciprocally regulated in primary astrocytes: association of GLT-1 with non-caveolar lipid rafts. *Glia.* 49:275–287.

48. Brown, D. A., and E. London. 1998. Structure and origin of ordered lipid domains in biological membranes. *J. Membr. Biol.* 164:103–114.

49. Schuck, S., M. Honsho, K. Ekroos, A. Shevchenko, and K. Simons. 2003. Resistance of cell membranes to different detergents. *Proc. Natl. Acad. Sci. USA.* 100:5795–5800.

50. Heerklotz, H. 2002. Triton promotes domain formation in lipid raft mixtures. *Biophys. J.* 83:2693–2701.

51. Kwik, J., S. Boyle, D. Fooksman, L. Margolis, M. P. Sheetz, and M. Edidin. 2003. Membrane cholesterol, lateral mobility, and the phosphatidylinositol 4,5-bisphosphate-dependent organization of cell actin. *Proc. Natl. Acad. Sci. USA.* 100:13964–13969.

52. Prior, I. A., C. Muncke, R. G. Parton, and J. F. Hancock. 2003. Direct visualization of Ras proteins in spatially distinct cell surface microdomains. *J. Cell Biol.* 160:165–170.

53. Parton, R. G. 1996. Caveolae and caveolins. *Curr. Opin. Cell Biol.* 8:542–548.

54. Parton, R. G., and A. A. Richards. 2003. Lipid rafts and caveolae as portals for endocytosis: new insights and common mechanisms. *Traffic.* 4:724–738.

55. Mineo, C., G. N. Gill, and R. G. Anderson. 1999. Regulated migration of epidermal growth factor receptor from caveolae. *J. Biol. Chem.* 274:30636–30643.

56. Prior, I. A., A. Harding, J. Yan, J. Sluimer, R. G. Parton, and J. F. Hancock. 2001. GTP-dependent segregation of H-ras from lipid rafts is required for biological activity. *Nat. Cell Biol.* 3:368–375.

57. Wilson, B. S., J. R. Pfeiffer, and J. M. Oliver. 2000. Observing FcepsilonRI signaling from the inside of the mast cell membrane. *J. Cell Biol.* 149:1131–1142.

58. Wilson, B. S., J. R. Pfeiffer, Z. Surviladze, E. A. Gaudet, and J. M. Oliver. 2001. High resolution mapping of mast cell membranes reveals primary and secondary domains of Fc(epsilon)RI and LAT. *J. Cell Biol.* 154:645–658.

59. Prior, I. A., R. G. Parton, and J. F. Hancock. 2003. Observing cell surface signaling domains using electron microscopy. *Sci. STKE.* 2003:PL9.

60. Frick, A., W. Zieglgansberger, and H. U. Dodt. 2001. Glutamate receptors form hot spots on apical dendrites of neocortical pyramidal neurons. *J. Neurophysiol.* 86:1412–1421.

61. Hering, H., C. C. Lin, and M. Sheng. 2003. Lipid rafts in the maintenance of synapses, dendritic spines, and surface AMPA receptor stability. *J. Neurosci.* 23:3262–3271.

62. Höchli, M., and C. R. Hackenbrock. 1976. Fluidity in mitochondrial membranes: thermotropic lateral translational motion of intramembrane particles. *Proc. Natl. Acad. Sci. USA.* 73:1636–1640.

63. Höchli, M., and C. R. Hackenbrock. 1977. Thermotropic lateral translational motion of intramembrane particles in the inner mitochondrial membrane and its inhibition by artificial peripheral proteins. *J. Cell Biol.* 72:278–291.

64. Maul, G. G. 1979. Temperature-dependent changes in intramembrane particle distribution. *In* Freeze Fracture: Methods, Artifacts, and Interpretation. J. E. Rash and C. S. Hudson, editors. Raven Press, New York. 37–42.

65. Hudson, C. S., J. E. Rash, and F. Graham. 1979. Introduction to sample preparation for freeze fracture. *In* Freeze Fracture: Methods, Artifacts, and Interpretation. J. E. Rash and C. S. Hudson, editors. Raven Press, New York. 1–10.

66. Quinn, P. J. 1985. A lipid-phase separation model of low-temperature damage to biological membranes. *Cryobiology.* 22:128–146.

67. Veatch, S. L., and S. L. Keller. 2002. Organization in lipid membranes containing cholesterol. *Phys. Rev. Lett.* 89:268101.

68. Dietrich, C., L. A. Bagatolli, Z. N. Volovyk, N. L. Thompson, M. Levi, K. Jacobson, and E. Gratton. 2001. Lipid rafts reconstituted in model membranes. *Biophys. J.* 80:1417–1428.

69. Anderson, R. G., and K. Jacobson. 2002. A role for lipid shells in targeting proteins to caveolae, rafts, and other lipid domains. *Science.* 296:1821–1825.

70. Simons, K., and G. van Meer. 1988. Lipid sorting in epithelial cells. *Biochemistry.* 27:6197–6202.

71. Canolle, B., F. Masmejean, C. Melon, A. Nieoullon, P. Pisano, and S. Lortet. 2004. Glial soluble factors regulate the activity and expression of the neuronal glutamate transporter EAAC1: implication of cholesterol. *J. Neurochem.* 88:1521–1532.

72. Tate, C. G., J. Haase, C. Baker, M. Boorsma, F. Magnani, Y. Vallis, and D. C. Williams. 2003. Comparison of seven different heterologous protein expression systems for the production of the serotonin transporter. *Biochim. Biophys. Acta.* 1610:141–153.

73. Magnani, F., C. G. Tate, S. Wynne, C. Williams, and J. Haase. 2004. Partitioning of the serotonin transporter into lipid microdomains modulates transport of serotonin. *J. Biol. Chem.* 279:38770–38778.

74. Eroglu, C., P. Cronet, V. Panneels, P. Beaufils, and I. Sinning. 2002. Functional reconstitution of purified metabotropic glutamate receptor expressed in the fly eye. *EMBO Rep.* 3:491–496.

75. Eroglu, C., B. Brugger, F. Wieland, and I. Sinning. 2003. Glutamate-binding affinity of Drosophila metabotropic glutamate receptor is modulated by association with lipid rafts. *Proc. Natl. Acad. Sci. USA.* 100:10219–10224.

76. Pike, L. J., X. Han, K. N. Chung, and R. W. Gross. 2002. Lipid rafts are enriched in arachidonic acid and plasmenylethanolamine and their composition is independent of caveolin-1 expression: a quantitative electrospray ionization/mass spectrometric analysis. *Biochemistry.* 41:2075–2088.